

Electronic Supplementary Information

Novel Octatungstate-Supported Tricarbonyl Metal Derivatives: $\{[H_2W_8O_{30}][M(CO)_3]_2\}^{8-}$ ($M = Mn^I$ and Re^I)

Jingyang Niu, Linping Yang, Junwei Zhao, Pengtao Ma and Jingping Wang*

Institute of Molecular and Crystal Engineering, College of Chemistry and Chemical Engineering, Henan University,
Kaifeng, Henan 475004, China

10

1. Experimental section.
2. Comments on previous reported typical organometallic derivatives of POMs.
3. UV-vis spectra. ity measure
4. The stabil ments of **1** and **3**.
- 15 5. IR spectra.

Fig. S1. (a) / (b) Comparison of the calculated and experimental XRD patterns of **1** and **3** in the angular range $2\theta = 5\text{--}40^\circ$ at 293 K.

Fig. S2. View of the 1D chain of **1**. Green octahedra: WO_6 unit.

20 Fig. S3. (a) Ball-and-stick representations of $\{[H_2W_8O_{30}][Re(CO)_3]_2\}^{8-}$ in **2**. (b) Polyhedral and ball-and-stick views of $\{[H_2W_8O_{30}][Re(CO)_3]_2\}^{8-}$ in **2**. Dark green octahedra: $\{W_3ReO_4\}$ cubanes. (The atoms with the suffix A is generated by the symmetry operation: A: $1 - x, 1 - y, 2 - z$)

Fig. S4. (a) View of the 2D window-like layer of **2** in the *ab* plane; (b) Schematic view of the 2D layer with (4, 4)-connected topology of **2**. All Na^+ ions and H_2O moleculars are omitted for clarity. Green octahedra: WO_6 unit.

25 Fig. S5. (a) Combined ball-and-stick representation of $[Na_2(H_2O)_6]^{2+}$ cations in **3**; (b) Combined ball-and-stick representation of a another type $[Na_2(H_2O)_6]^{2+}$ dimeric in **3**; (c) Ball-and-stick representation of $[Na_4(H_2O)_{10}]^{4+}$ cluster in **3**. Color code: Cambridge blue, sodium atom; red, oxygen atom. (The atoms with the suffix A, B, C and D are generated by the symmetry operation: A: $2 - x, 2 - y, 2 - z$; B: $2 - x, 3 - y, 2 - z$; C: $x, 1 + y, z$; D: $2 - x, 2 - y, 3 - z$)

Fig. S6. (a) Ball-and-stick illustration of the polyoxoanion $\{Mo_6O_{16}(OCH_3)_2[HOCH_2C(CH_2O)_3]_2[Mn(CO)_3]_2\}^{2-}$.

30 Fig. S7. The UV-vis spectra of **1** and **3** in the mixed solvent of CH_3CN / H_2O (1: 2, volume ratio).

Fig. S8. The UV-vis spectra recorded during the titration of $Mn(CO)_5Br$ in acetonitrile.

Fig. S9. Comparison of the CV curves of **1** and **3** in the mixed solvent of CH_3CN / Na_2SO_4 ($0.5 \text{ mol}\cdot L^{-1}$) (1: 2, volume ratio). A 3 mm diameter glassy carbon disk electrode (GCE) was used as a working electrode, a platinum wire served as the counter electrode and an Hg/Hg_2Cl_2 electrode as the reference electrode.

35 Fig. S10. (a) / (b) The CV curves of **1** / **3** in the mixed solvent of $CH_3CN / Na_2SO_4(0.5 \text{ mol}\cdot L^{-1})$ (1: 2, volume ratio) at different scan rates (from inner to outer: 50, 100, 150, 200, 250, 300, 350, 400, 450, 500, 550, 600 mVs^{-1}); (c) / (d) The

variation of the CV cathodic peak currents with increasing scan rates from 50 to 600 mVs⁻¹ of **1** / **3**. A 3 mm diameter glassy carbon disk electrode (GCE) was used as a working electrode, a platinum wire served as the counter electrode and an Hg/Hg₂Cl₂ electrode as the reference electrode.

Fig. S11. (a) / (b) The aging of the solution of **1** / **3** detected by the *in-situ* UV-vis spectra.

Fig. S12. (a) The UV-vis spectral evolution of **1** in the alkaline direction; (b) The UV-vis spectral evolution of **1** in the acidic direction; (c) The UV-vis spectral evolution of **3** in the alkaline direction; (d) The UV-vis spectral evolution of **3** in the acidic direction.

Fig. S13. (a) The UV-vis spectral evolution of Na₂WO₄·2H₂O in the alkaline direction; (b) The UV-vis spectral evolution of Na₂WO₄·2H₂O in the acidic direction. (The pH value of Na₂WO₄·2H₂O that was dissolved in the mixed solution (8×10^{-5} mol·L⁻¹) was 5.70.)

Fig. S14. (a) The CV curves evolution of **1** in the alkaline direction; (b) The CV curves evolution of **1** in the acidic direction; (c) The CV curves evolution of **3** in the alkaline direction; (d) The CV curves evolution of **3** in the acidic direction. The pH value of **1** and **3** were dissolved in the mixed solvent of CH₃CN / Na₂SO₄(0.5 mol·L⁻¹) (1: 2, volume ratio) are 5.75 and 5.77, respectively. Scan rate: 100 mV·s⁻¹. The pH values are adjusted using diluted HCl or NaOH solution. A 3 mm diameter glassy carbon disk electrode (GCE) was used as a working electrode, a platinum wire served as the counter electrode and an Hg/Hg₂Cl₂ electrode as the reference electrode.

Fig. S15. IR spectrum of Mn(CO)₅Br.

Fig. S16. IR spectra of compound **1**–**3**.

1. Experimental section:

Preparation of 1. Mn(CO)₅Br (0.137 g, 0.498 mmol) in 7.0 mL CH₃OH was refluxed in the dark for 1 h and then cooled to room temperature (**A**). Na₂WO₄·2H₂O (4.950 g, 15.00 mmol) was dissolved in 10 mL distilled water and 0.75 mL acetic acid was added. The resulting suspension was boiled for 30 min and then cooled to room temperature (**B**). Then **A** was added dropwise into **B** at 25 °C, and the mixed solution was stirred in the dark for half an hour, cooled and filtered. The filtrate was allowed to stand at room temperature in the dark place for slow evaporation. Orange block crystals of **1** were isolated after some days. (Yield: *ca* 35% based on Mn(CO)₅Br). Elemental analysis (%) calcd for **1**: C, 2.67; H, 2.02; found: C, 2.72; H, 2.13. IR (KBr pellet): 2022(s), 1932(s), 1636(s), 920(m), 881(sh), 824(s), 759(s), 668(w), 597(m), 552(m) cm⁻¹ (Fig. S16†).

Preparation of 2. The synthetic process was used with Re(CO)₅Br (0.203 g, 0.499 mmol) replacing Mn(CO)₅Br (0.137 g, 0.498 mmol). Yellowish green block carstals of **2** were obtained. (Yield: *ca* 20% based on Re(CO)₅Br). Elemental analysis (%) calcd for **2**: C, 2.38; H, 1.60; found: C, 2.46; H, 1.68. IR (KBr pellet): 2007(s), 1885(s), 1635(s), 927(m), 890(sh), 822(s), 768(s), 671(w), 586(m), 566(m) cm⁻¹ (Fig. S16†).

Preparation of 3. Mn(CO)₅Br (0.137 g, 0.498 mmol) in 7.0 mL CH₃CN was refluxed in the dark for 1 h and then cooled to room temperature. (**A**). Na₂WO₄·2H₂O (4.950 g, 15.00 mmol) was dissolved in 10 mL distilled water and 0.75 mL acetic acid was added. Then the colorless solution was boiled for 10 min. Then a solution of Mn(Ac)₂·4H₂O (0.613 g, 2.500 mmol) and 0.02 mL acetic acid in 3 mL water was added dropwise. The resulting suspension was boiled for 20 min, cooled and filtered (**B**). Then **A** was added dropwise into **B** at 25 °C with gentle stirring and the mixed solution was stirred in the dark for half an hour, cooled and filtered. Yellow needle-like crystals of **3** were found after 1-2 weeks. (Yield: *ca*

38% based on $\text{Mn}(\text{CO})_5\text{Br}$). Elemental analysis (%) calcd for 3: C, 2.52; H, 1.76; found: C, 2.36; H, 1.89. IR (KBr pellet): 2026(s), 1927(s), 1636(s), 924(m), 850(s), 821(sh), 735(s), 594(m), 552(m) cm^{-1} (Fig. S16†).

Synthetic discussion. It is difficult to prepare POM-based carbonyl metal derivatives owing to the chemical inertness and instability of carbonyl metal compounds. Based on previous literatures, most of known POM-supported tricarbonyl metal compounds are discrete structure and mainly focus on the polyoxomolybdate-supported manganese carbonyl. To our knowledge, isopolyoxotungstate(IPOTs)-based carbonyl metal compounds have never been synthesized. These ignited our intensive interest in obtaining novel carbonyl metal derivatives of IPOTs with multidimensional structures. Instead of using the IPOT precursors, we directly employed Na_2WO_4 to react with $\text{Mn}(\text{CO})_5\text{Br}$ / $\text{Re}(\text{CO})_5\text{Br}$. The structures of **1** and **2** are discrete, in order to obtain extended structures containing $\{[\text{H}_2\text{W}_8\text{O}_{30}][\text{Mn}(\text{CO})_3]_2\}^{8-}$ unit, by introducing $\text{Mn}(\text{Ac})_2 \cdot 4\text{H}_2\text{O}$ to the reaction system, finally, the 1D chain **3** was prepared..

2. Comments on previous reported typical organometallic derivatives of POMs:

Though carbonyl metal derivatives of POMs have attracted increasing interest in the recent years, the reports on new types of POM-based carbonyl metal derivatives are very rare, which is related to three main reasons: Firstly, most polyoxoanions have not enough charge density to combine with carbonyl metal groups. Moreover, carbonyl metal compounds are easy to decompose on heating or irradiation. Secondly, the solubility of polyoxoanions differs greatly from that of carbonyl compounds in the same kind of solvent. Thirdly, carbonyl metal compounds are very expensive.

At the present time, the reported POM-supported carbonyl metal derivatives are mainly concentrated on Lindqvist-type polyoxoanions and Dawson-type $[\text{P}_2\text{W}_{15}\text{Nb}_3\text{O}_{62}]^{9-}$ polyoxoanions. The first POM-supported carbonyl metal compounds $[(\text{OC})_3\text{M}(\text{Nb}_2\text{W}_4\text{O}_{19})]^{3-}$ ($\text{M} = \text{Mn, Re}$) were obtained by Klemperer' group in 1980.¹ Although they did not have crystal structure characterization, they forecasted their structures by the ^{17}O NMR study, and their structures was proved in 1985.² The $[\text{M}(\text{CO})_3]^+$ ($\text{M} = \text{Mn, Re}$) group is bonded to three adjacent bridging oxygens of the $[\text{Nb}_2\text{W}_4\text{O}_{19}]^{4-}$ polyoxoanion. At the same time, Day and Klemperer reported a series of Lindqvist-polyoxoanion-supported carbonyl metal compounds.³ A typical example is $[(\eta^5\text{-C}_5\text{H}_5)\text{Ti}(\text{Mo}_5\text{O}_{18})\text{Mn}(\text{CO})_3]^{2-}$,^{3b} in which a $[\text{Mn}(\text{CO})_3]^+$ unit is bonded to three bridging oxygen atoms of the $[(\eta^5\text{-C}_5\text{H}_5)\text{Ti}(\text{Mo}_5\text{O}_{18})]^{3-}$ anion. It is worthwhile to note that the compound contains $[(\eta^5\text{-C}_5\text{H}_5)\text{Ti}]^{3+}$ and $[\text{Mn}(\text{CO})_3]^+$ two organic groups. In 1997, Finke *et al.* prepared a few $[\text{P}_2\text{W}_{15}\text{Nb}_3\text{O}_{62}]^{9-}$ -supported carbonyl metal compounds: $[(n\text{-C}_4\text{H}_9)_4\text{N}]_8[\text{Re}(\text{CO})_3\text{P}_2\text{W}_{15}\text{Nb}_3\text{O}_{62}] \cdot (n\text{-C}_4\text{H}_9)_4\text{NBF}_4$, $[(n\text{-C}_4\text{H}_9)_4\text{N}]_8[\text{Ir}(\text{CO})_2\text{P}_2\text{W}_{15}\text{Nb}_3\text{O}_{62}]$ and $[(n\text{-C}_4\text{H}_9)_4\text{N}]_8[\text{Rh}(\text{CO})_2\text{P}_2\text{W}_{15}\text{Nb}_3\text{O}_{62}]$.⁴ In 2001, Pope *et al.* found this type of compounds based on isoniobate or isotantalate: $\text{K}_7[\text{M}_6\text{O}_{19}\text{M}'(\text{CO})_3]$ ($\text{M} = \text{Nb, Ta}; \text{M}' = \text{Mn, Re}$) and $\{\text{M}_6\text{O}_{19}[\text{M}'(\text{CO})_3]_2\}^{6-}$ ($\text{M} = \text{Nb, Ta}; \text{M}' = \text{Mn, Re}$).⁵ In 2003, Gouzerh *et al.* reported several compounds containing $[\text{Mo}_5\text{O}_{13}(\text{OMe})_4(\text{NO})]^{3-}$ and $[\text{M}(\text{CO})_3]^+$ ($\text{M} = \text{Mn, Re}$) units.⁶ Take $(n\text{Bu}_4\text{N})_2[\text{Re}(\text{CO})_3(\text{H}_2\text{O})]$ and $(n\text{Bu}_4\text{N})_3\{\text{Na}[\text{Mo}_5\text{O}_{13}(\text{OMe})_4(\text{NO})]_2[\text{Mn}(\text{CO})_3]_2\}$ for instance, in the former, The $[\text{Re}(\text{CO})_3]^+$ fragment is bonded to two adjacent axial oxygen atoms of the $[\text{Mo}_5\text{O}_{13}(\text{OMe})_4(\text{NO})]$ unit and a water molecule whereas the latter consists of two crystallographically independent $\{[\text{Mo}_5\text{O}_{13}(\text{OMe})_4(\text{NO})][\text{Mn}(\text{CO})_3]\}^{2-}$ units linked by a sodium cation. In 2008, our group synthesized a new compound $(n\text{-Bu}_4\text{N})_2\{\text{Mo}_6\text{O}_{16}(\text{OCH}_3)_2[\text{HOCH}_2\text{C}(\text{CH}_2\text{O})_3]_2[\text{Mn}(\text{CO})_3]_2\}$ (Fig. S6)⁷. In summary, the bonding of the $[\text{M}(\text{CO})_3]^+$ ($\text{M} = \text{Mn}^{\text{I}}, \text{Re}^{\text{I}}$) fragment, as a $d^6\text{-fac-ML}_3$ unit to a triangle of connecting three oxygen atoms, is common in POM-supported organometallic compounds.¹⁻⁸

- [1] C. J. Besecker and W. G. Klemperer, *J. Am. Chem. Soc.*, 1980, **102**, 7598.
- [2] C. J. Besecker, V. W. Day, W. G. Klemperer and M. R. Thompson, *Inorg. Chem.*, 1985, **24**, 44.
- [3] (a) W. G. Klemperer and D. J. Main, *Inorg. Chem.*, 1990, **29**, 2355; (b) W. G. Day, M. F. Fredrich, M. R. Thompson, W. G. Klemperer, R. S. Liu and W. Shum, *J. Am. Chem. Soc.*, 1981, **103**, 3597; (c) W. G. Klemperer and B. Zhong, *Inorg. Chem.*, 1993, **32**, 5821.
- [4] T. Nagata, M. Pohl, H. Weiner and R. G. Finke, *Inorg. Chem.*, 1997, **36**, 1366.
- [5] A. V. Besserguenev, M. H. Dickman and M. T. Pope, *Inorg. Chem.*, 2001, **40**, 2582.
- [6] R. Villanneau, A. Proust, F. Robert and P. Gouzerh, *Chem. Eur. J.*, 2003, **9**, 1982.
- [7] J. P. Wang, J. L. Li and J. Y. Niu, *Chemical Research in Chinese University*, 2008, **24**, 675.
- [8] (a) V. W. Day and R. G. Klemperer, *Polyoxometalates: From Platonic Solids to Anti-Retroviral Activity* (Eds.: M. T. Pope and A. Müller), Kluwer, Dordrecht, 1994, pp. 87; (b) A. V. Besserguenev, M. H. Dickman and M. T. Pope, *Inorg. Chem.*, 2001, **40**, 2582.

3. UV-vis spectra:

The UV-vis spectra of **1** and **3** in the mixed solvent of CH₃CN / H₂O (1: 2, volume ratio) in the region of 190–500 nm (Fig. S7), all display two similar absorption bands at 200 and 364 nm for **1**, 200 and 366 nm for **3**, respectively. The higher one can be corresponded to the charge transfer transitions of the O_t → W bonds,¹ suggesting the presence of polyoxoanions; while the lower one can be assigned to π→π* transitions which is not obvious resulting from the lower concentration,² indicating the existence of [Mn(CO)₃]⁺.

- [1] J. Y. Niu, J. P. Wang, *Introduction of Heteropoly Compounds*. Henan University Press: Kaifeng, 2000.
- [2] (a) D. Burdinski, E. Bothe and K. Wieghardt, *Inorg. Chem.*, 2000, **39**, 105; (b) M. Busby, P. Matousek, M. Towrie, I. P. Clark, M. Motlevalli, F. Hartl and A. Jr. Vlček, *Inorg. Chem.*, 2004, **43**, 4523; (c) S. Y. Reece and D. G. Nocera, *J. Am. Chem. Soc.*, 2005, **127**, 9448; (d) H. D. Batey, A. C. Whitwood and A. K. Duhme-Klair, *Inorg. Chem.*, 2007, **46**, 6516.

4. The stability measurements of **1** and **3**:

To investigate the influences of the pH on the stability of the compounds in the mixed solvent of CH₃CN / H₂O (1: 2, volume ratio), in situ UV-vis spectroscopic measurements of **1** and **3** were performed in this mixed solution (Fig. S12). The pH values in the acidic direction were adjusted using diluted HCl solution while the pH values in the alkaline direction were adjusted using diluted NaOH solution. The pH value of **1** that was dissolved in the mixed solution (1×10^{-5} mol·L⁻¹) was 5.53, and the pH value of **3** that was dissolved in the mixed solution (1×10^{-5} mol·L⁻¹) was 5.42.

As shown in Fig. S12a, the UV-vis spectra of **1** in the mixed solution display a cuspidal absorption band at about 200 nm at pH = 5.53. With the pH value increasing, the absorption band at ca. 200 nm is gradually blue-shifted whereas the absorbance become larger, indicating that **1** may be gradually decomposed to WO₄²⁻ ions, which are testified to the UV-vis spectral evolution of the diluted Na₂WO₄·2H₂O in the alkaline solution (Fig. S13a). A conclusion can be drawn that the skeleton of **1** has been destroyed at the pH higher than 7.5. In contrast, when the pH value decreasing (Fig. S12b), the absorption band at ca. 200 nm is gradually red-shifted and more and more weak, meanwhile, the new absorption band at ca.

260 nm appears assigned to the $O_{b,c} \rightarrow W$ charge transfer transitions, which is possibly credited to the polymerization of WO_4^{2-} ions upon addition of diluted HCl solution (Fig. S13b). In a word, when the pH values are lower than 5.0 or higher than 7.5, the UV-vis spectra change strikingly, suggesting that the polyoxoanion have been polymerized or decomposed. The above analyses show that the pH stable range of **1a** in the mixed solution is about 5.0–7.5. In addition, the evolution processes of CV curves of **1** at different pH values can also give a complementary proof of the stability in the larger pH ranges. As depicted in Fig. S14a and S14b, when the pH values vary in the range of 5.0–7.5, the peak shapes and positions of the redox waves slightly change, suggesting that the $[(H_2W_8O_{30})\{Mn(CO)_3\}_2]^{8-}$ cluster is still retained, which is in good agreement with the results of UV-vis spectra.

The influences of the pH value on the stability of **3** in the mixed solution are similar to **1**. As detailed shown in Fig. S12c₁₀ and S12d, we presume that the pH stable range of **1a** in **3** in the mixed solution is about 5.0–7.5, which is corresponded to the evolution of CV curves of **3** at different pH conditions (Fig. S14c and S14d,).

5. IR spectra:

IR spectra in the 400–4000 cm^{-1} region of **1** and **3** are similar; indicating the structural type of the polyoxoanions is similar, which are in good agreement with the results of X-ray diffraction structural analyses (Fig. S15 and S16). In IR₁₅ spectra of **1** and **3**, two bands are observed at *ca.* 1900 and 2000 cm^{-1} , which correspond to the carbonyl stretching vibration of a C_{3v} metal tricarbonyl unit.¹ The 700–1000 cm^{-1} region show the stretching vibration of W–O bonds from the $[H_2W_8O_{30}]^{10-}$ isopolyoxotungstate.

[1] (a) E. W. Abel and G. Wilkinson, *J. Chem. Soc.*, 1959, 1501; (b) W. J. Kirkham, A. J. Osborne, R. S. Nyholm and M. H. B. Stiddard, *J. Chem. Soc.*, 1965, 551; (c) C. S. Kraihanzel and P. K. Maples, *J. Organomet. Chem.*, 1976, **117**, 159; (d) R. Villanneau, R. Delmont, A. Proust and P. Gouzerh, *Chem. Eur. J.*, 2000, **6**, 1184; (e) A. V. Besserguenev, M. H. Dickman and M. T. Pope, *Inorg. Chem.*, 2001, **40**, 2582; (f) R. Villanneau, A. Proust, F. Robert and P. Gouzerh, *Chem. Eur. J.*, 2003, **9**, 1982.

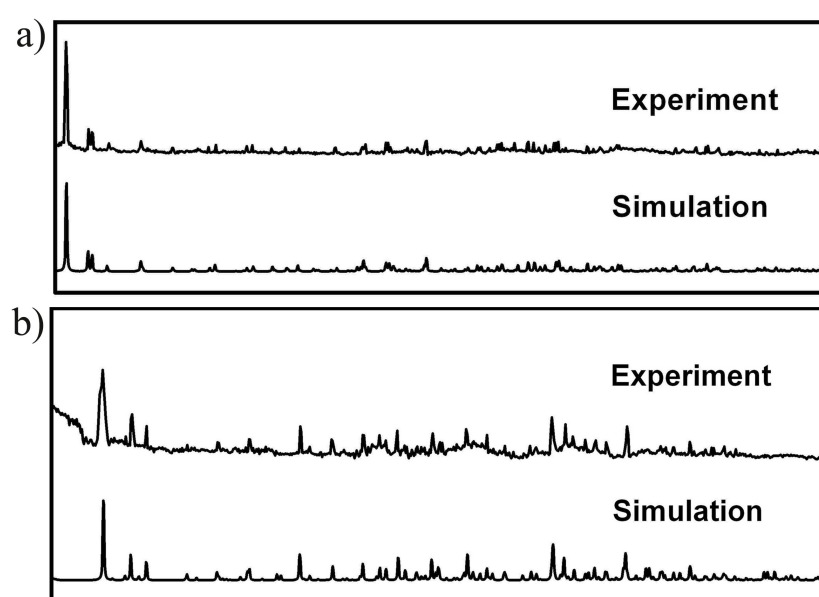


Fig. S1. (a) / (b) Comparison of the calculated and experimental XRD patterns of **1** and **3** in the angular range $2\theta = 5\text{--}40^\circ$ at 293 K.

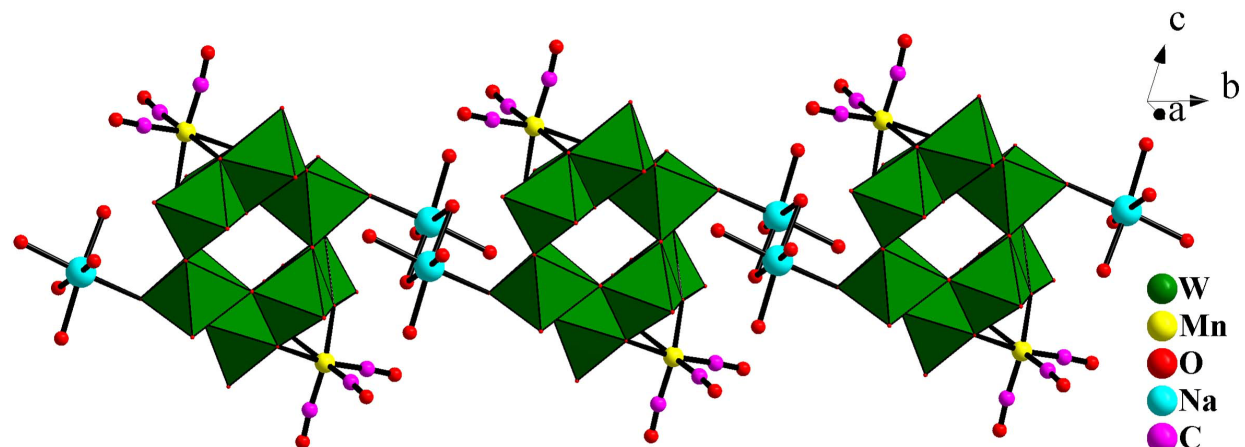


Fig. S2. View of the 1D chain of **1**. Green octahedra: WO_6 unit.

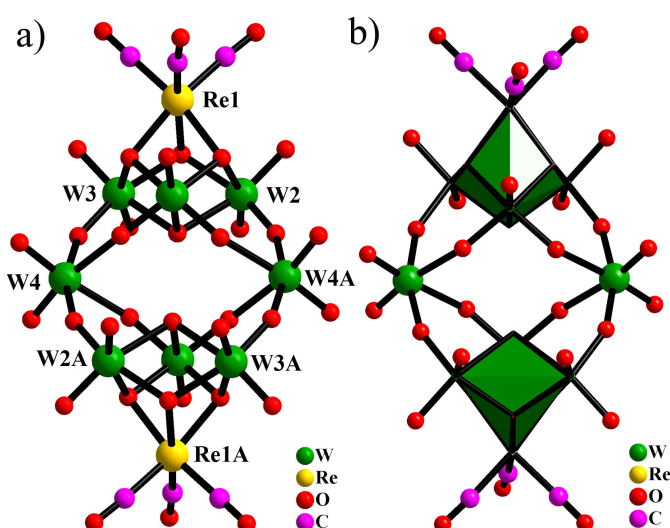


Fig. S3. (a) Ball-and-stick representations of $\{\text{H}_2\text{W}_8\text{O}_{30}\}[\text{Re}(\text{CO})_3]_2\}^{8-}$ in **2**. (b) Polyhedral and ball-and-stick views of $\{\text{H}_2\text{W}_8\text{O}_{30}\}[\text{Re}(\text{CO})_3]_2\}^{8-}$ in **2**. Dark green octahedra: $\{\text{W}_3\text{ReO}_4\}$ cubanes. (The atoms with the suffix A is generated by the symmetry operation: A: $1 - x, 1 - y, 2 - z$)

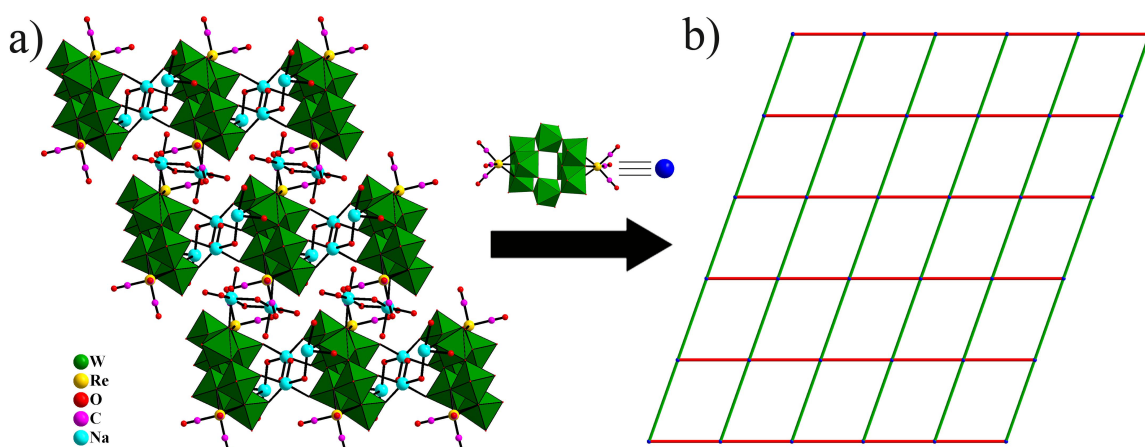


Fig. S4. (a) View of the 2D window-like layer of **2** in the *ab* plane; (b) Schematic view of the 2D layer with (4, 4)-connected topology of **2**. All Na^+ ions and H_2O molecules are omitted for clarity. Green octahedra: WO_6 unit.

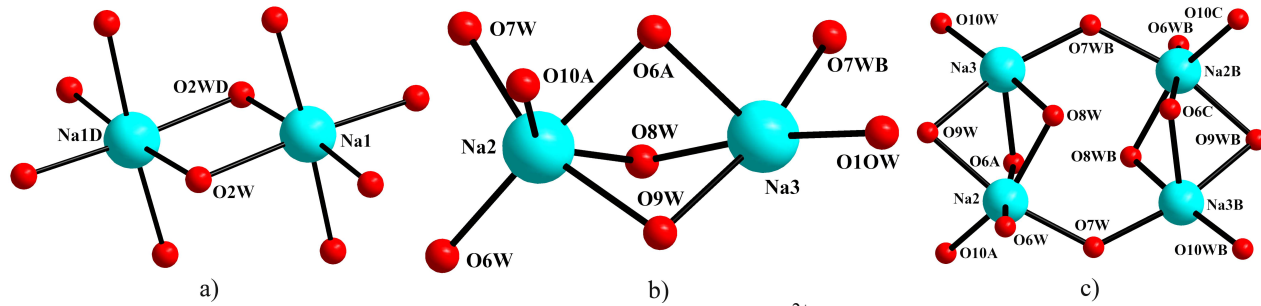


Fig. S5. (a) Combined ball-and-stick representation of $[\text{Na}_2(\text{H}_2\text{O})_6]^{2+}$ cations in **3**; (b) Combined ball-and-stick representation of another type $[\text{Na}_2(\text{H}_2\text{O})_6]^{2+}$ dimeric in **3**; (c) Ball-and-stick representation of $[\text{Na}_4(\text{H}_2\text{O})_{10}]^{4+}$ cluster in **3**. Color code: Cambridge blue, sodium atom; red, oxygen atom. (The atoms with the suffix A, B, C and D are generated by the symmetry operation: A: $2 - x, 2 - y, 2 - z$; B: $2 - x, 3 - y, 2 - z$; C: $x, 1 + y, z$; D: $2 - x, 2 - y, 3 - z$)

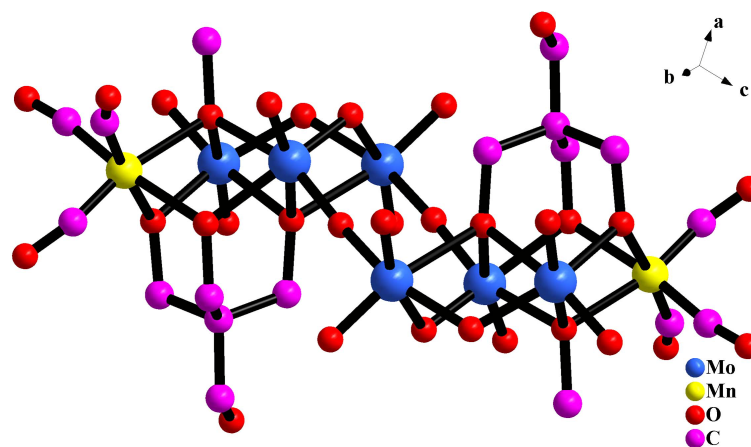


Fig. S6. (a) Ball-and-stick illustration of the polyoxoanion $\{\text{Mo}_6\text{O}_{16}(\text{OCH}_3)_2[\text{HOCH}_2\text{C}(\text{CH}_2\text{O})_3]_2[\text{Mn}(\text{CO})_3]_2\}^{2-}$.

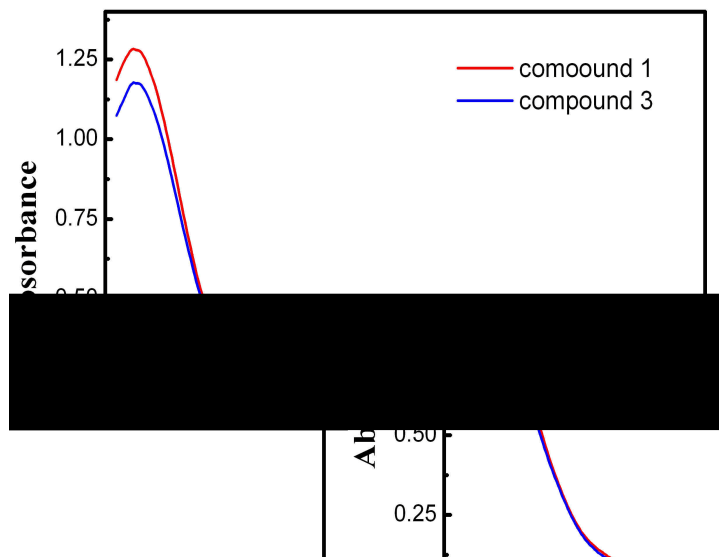


Fig. S7. The UV-vis spectra of **1** and **3** in the mixed solvent of CH₃CN / H₂O (1: 2, volume ratio).

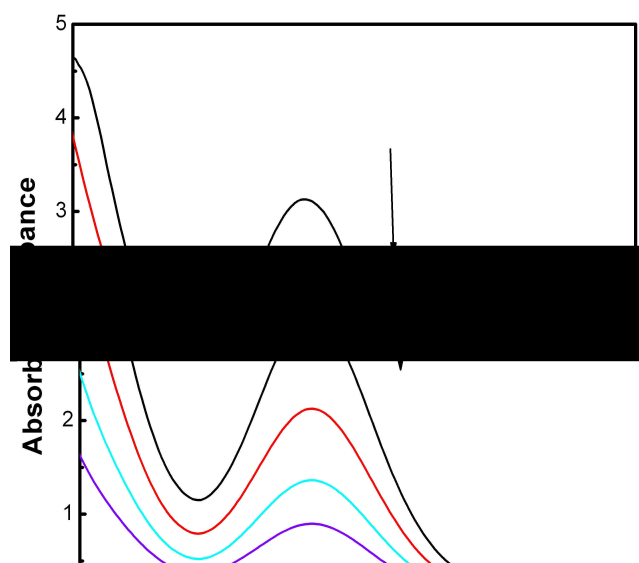


Fig. S8. The UV-vis spectra recorded during the titration of $\text{Mn}(\text{CO})_5\text{Br}$ in acetonitrile.

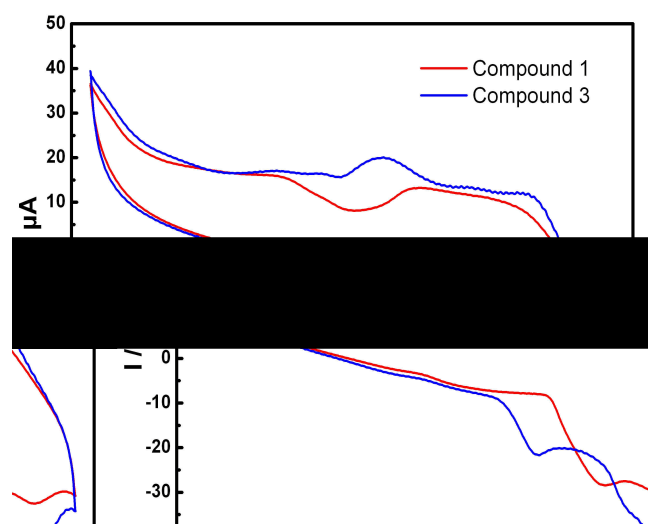


Fig. S9. Comparison of the CV curves of **1** and **3** in the mixed solvent of $\text{CH}_3\text{CN} / \text{Na}_2\text{SO}_4(0.5 \text{ mol}\cdot\text{L}^{-1})$ (1: 2,

Table S1 The reduction peak E_{pc} , oxidation peak E_{pa} and peak-to-peak separation ΔE_p of **1** and **3**

| Compound | $E_{pc}[\text{V}]$ | $E_{pa}[\text{V}]$ | $\Delta E_p[\text{mV}]$ |
|----------|--------------------|--------------------|-------------------------|
| 1 | -0.401 | | |
| | -0.331 | 0.790 | 459 |
| 3 | | | 1.184 |
| | 0.167 | 0.437 | 270 |
| | 0.940 | 1.180 | 240 |

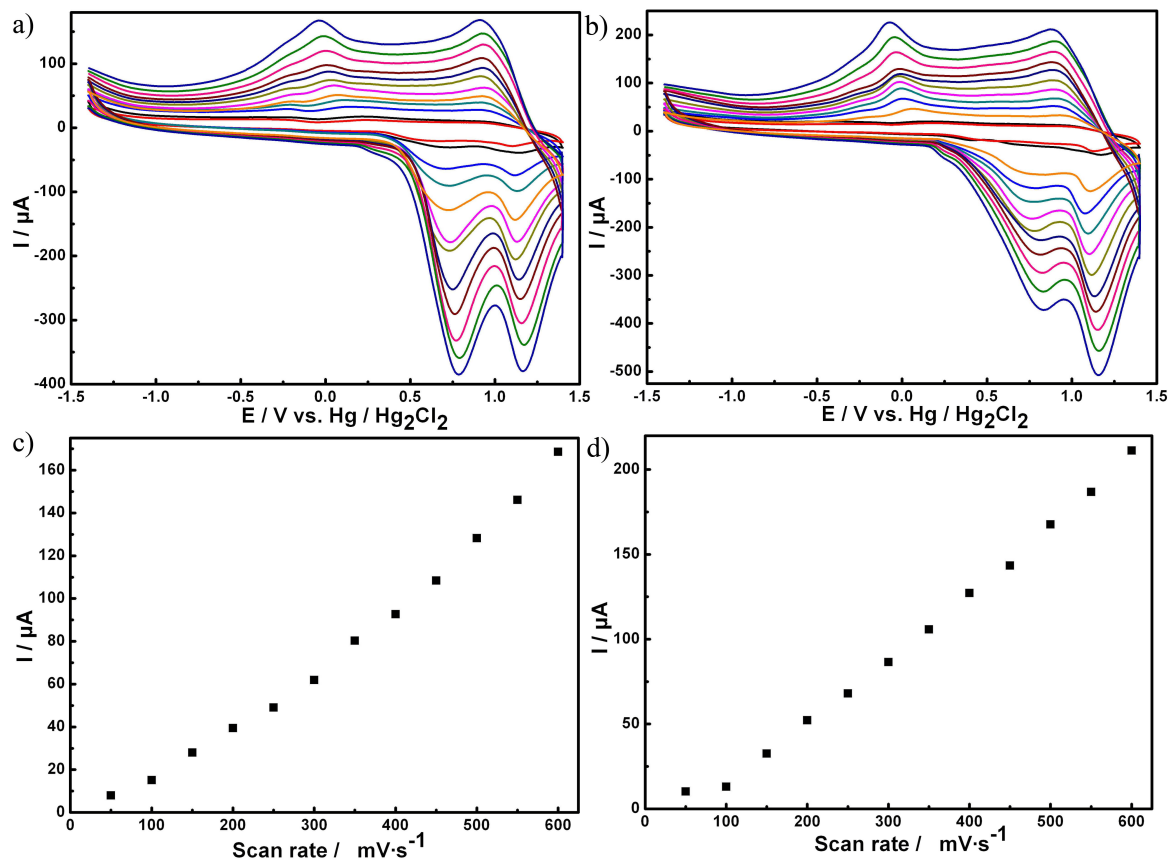


Fig. S10. (a) / (b) The CV curves of **1** / **3** in the mixed solvent of $\text{CH}_3\text{CN} / \text{Na}_2\text{SO}_4 (0.5 \text{ mol L}^{-1})$ (1:2, volume ratio), at different scan rates (from inner to outer: 50, 100, 150, 200, 250, 300, 350, 400, 450, 500, 550, 600 mV s^{-1}); (c) / (d) The variation of the CV cathodic peak currents with increasing scan rates from 50 to 600 mV s^{-1} of **1** / **3**. A 3 mm diameter glassy carbon disk electrode (GCE) was used as a working electrode, a platinum wire served as the counter electrode and an $\text{Hg}/\text{Hg}_2\text{Cl}_2$ electrode as the reference electrode.

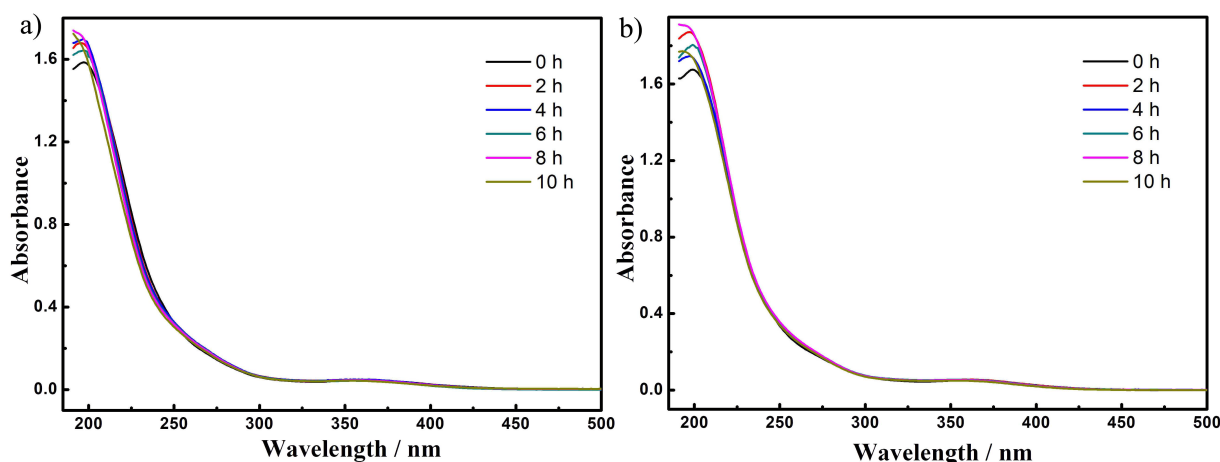


Fig. S11. (a) / (b) The aging of the solution of **1** / **3** detected by the *in-situ* UV-vis spectra.

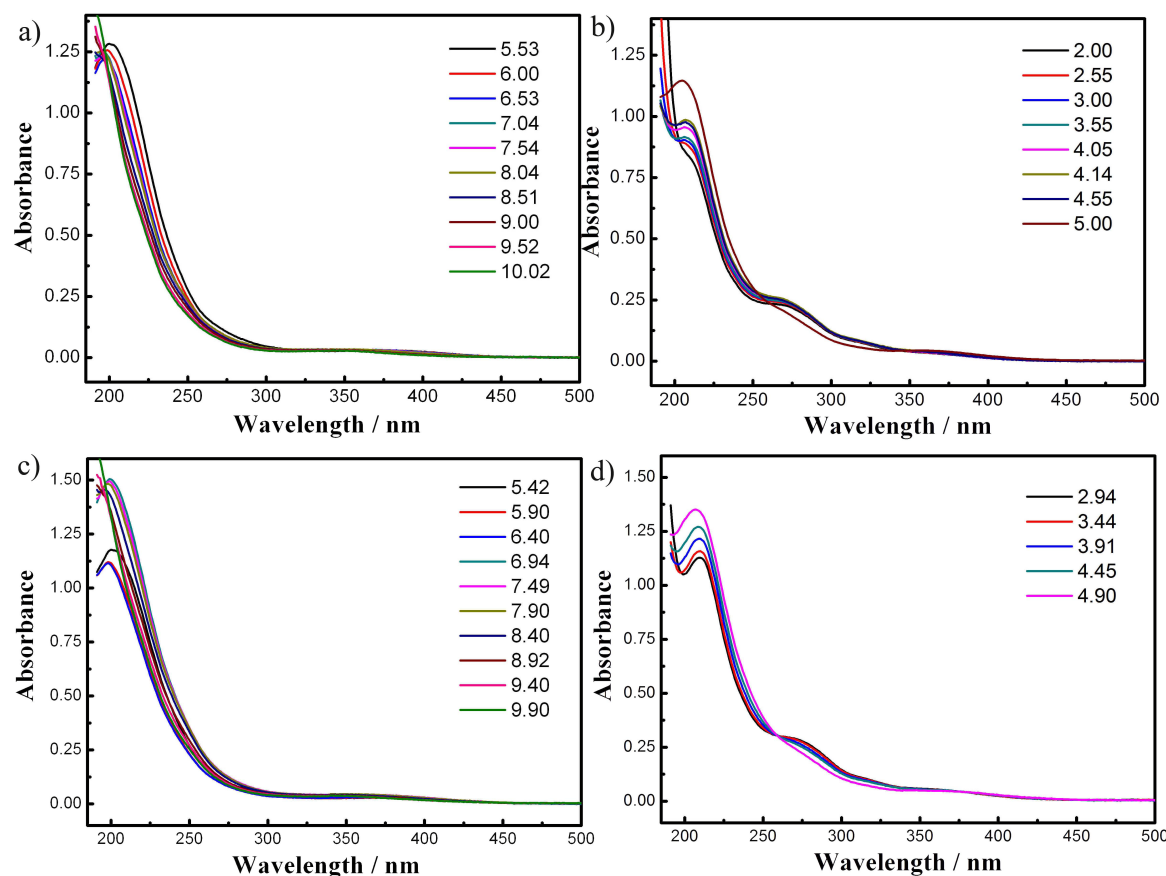


Fig. S12. (a) The UV-vis spectral evolution of **1** in the alkaline direction; (b) The UV-vis spectral evolution of **1** in the acidic direction; (c) The UV-vis spectral evolution of **3** in the alkaline direction; (d) The UV-vis spectral evolution of **3** in the acidic direction.

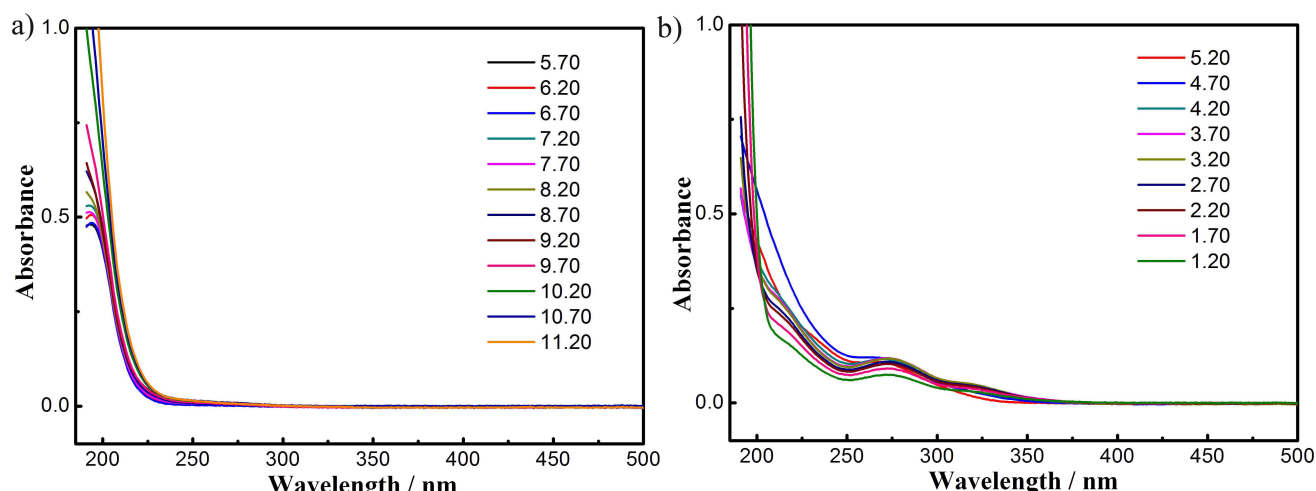


Fig. S13. (a) The UV-vis spectral evolution of $\text{Na}_2\text{WO}_4 \cdot 2\text{H}_2\text{O}$ in the alkaline direction; (b) The UV-vis spectral evolution of $\text{Na}_2\text{WO}_4 \cdot 2\text{H}_2\text{O}$ in the acidic direction. (The pH value of $\text{Na}_2\text{WO}_4 \cdot 2\text{H}_2\text{O}$ that was dissolved in the mixed solution ($8 \times 10^{-5} \text{ mol} \cdot \text{L}^{-1}$) was 5.70.)

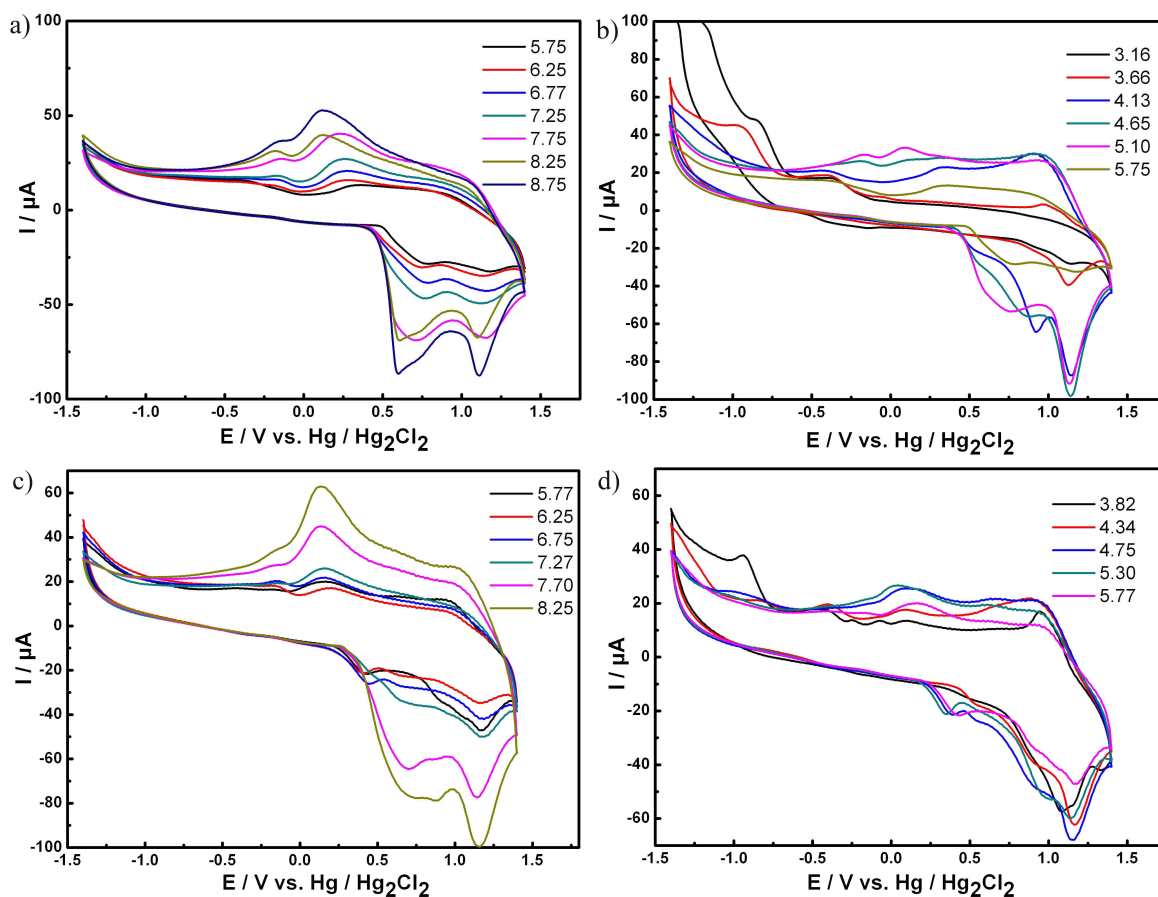


Fig. S14. (a) The CV curves evolution of **1** in the alkaline direction; (b) The CV curves evolution of **1** in the acidic direction; (c) The CV curves evolution of **3** in the alkaline direction; (d) The CV curves evolution of **3** in the acidic direction. The pH value of **1** and **3** were dissolved in the mixed solvent of $\text{CH}_3\text{CN} / \text{Na}_2\text{SO}_4(0.5 \text{ mol} \cdot \text{L}^{-1})$ (1: 2, volume ratio) are 5.75 and 5.77, respectively. Scan rate: $100 \text{ mV} \cdot \text{s}^{-1}$. The pH values are adjusted using diluted HCl or NaOH solution. A 3 mm diameter glassy carbon disk electrode (GCE) was used as a working electrode, a platinum wire served as the counter electrode and an $\text{Hg} / \text{Hg}_2\text{Cl}_2$ electrode as the reference electrode.

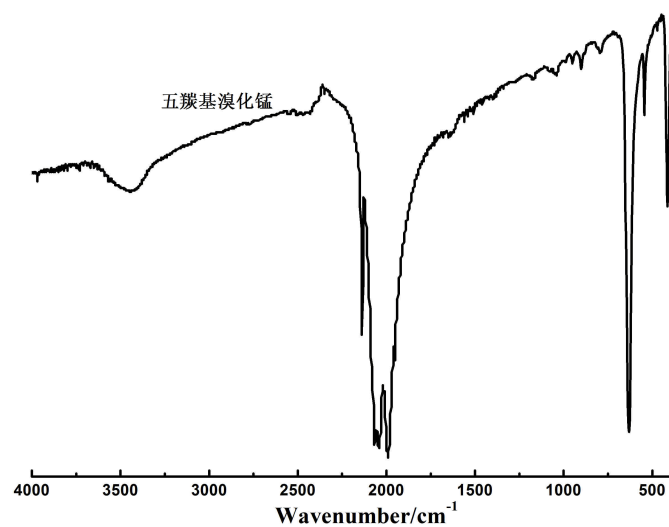


Fig. S15. IR spectrum of $\text{Mn}(\text{CO})_5\text{Br}$.

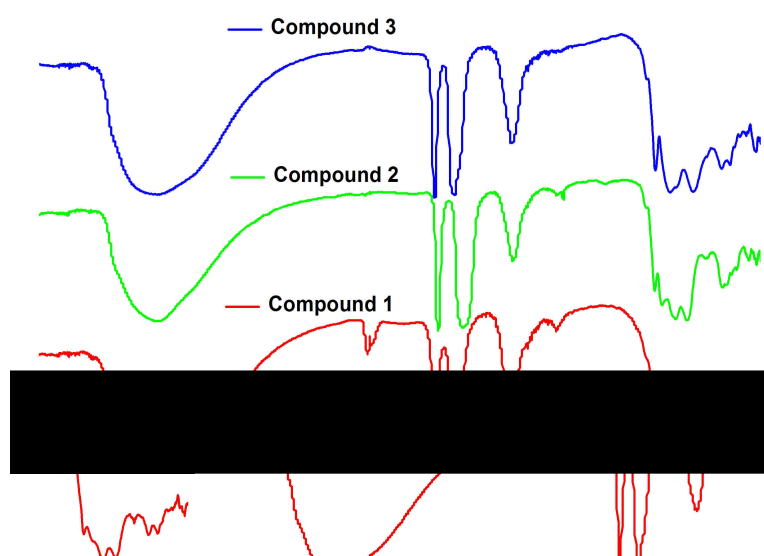


Fig. S16. IR spectra of compound 1–3.